Original Article

Efficacy of Adjunctive Tofacitinib Therapy in Mouse Models of Tuberculosis

Mamoudou Maiga [a,b,1], Bintou Ahmadou Ahidjo [a,c], Mariama C. Maiga [a,c], Laurene Cheung [a,c], Shaaretha Pelly [a,c], Shichun Lun [a], Flabou Bougoudogo [b], William R. Bishai [a,c,*]

[a] Center for Tuberculosis Research, Johns Hopkins University School of Medicine, Baltimore, MD, USA
[b] Université des Sciences, des Techniques et des Technologies de Bamako (USTTB), Bamako, Mali
[c] Howard Hughes Medical Institute, Chevy Chase, MD, USA

ARTICLE INFO

ABSTRACT

The global tuberculosis (TB) epidemic and the spread of multi- and extensively-drug resistant strains of *Mycobacterium tuberculosis* (*M.tb*) have been fueled by low adherence to following lengthy treatment protocols, and the rapid spread of HIV (Human Immunodeficiency Virus). Persistence of the infection in immunocompetent individuals follows from the ability of *M.tb* to subvert host immune responses in favor of survival within macrophages. Alternative host-directed strategies are therefore being currently sought to improve treatment efficacy and duration. In this study, we evaluated tofacitinib, a new oral Janus kinase (JAK) blocker with anti-inflammatory properties, in shortening tuberculosis treatment. BALB/c mice, which are immunocompetent, showed acceleration of *M.tb* clearance achieving apparent sterilization after 16 weeks of adjunctive tofacitinib therapy at average exposures higher than recommended in humans, while mice receiving standard treatment alone did not achieve clearance until 24 weeks. True sterilization with tofacitinib was not achieved until five months. C3HeB/FeJ mice, which show reduced pro-inflammatory cytokines during *M.tb* infection, did not show improved clearance with adjunctive tofacitinib therapy, indicating that the nature of granulomatous lesions and host immunity may influence responsiveness to tofacitinib. Our findings suggest that the JAK pathway could be explored further for host-directed therapy in immunocompetent individuals.

© 2015 The Authors. Published by Elsevier B.V. This is an open access article under the CC BY-NC-ND license (http://creativecommons.org/licenses/by-nc-nd/4.0/).

1. Introduction

Tuberculosis (TB) claims 1.6 million lives every year. Efforts to control the global epidemic are further undermined by an ever-increasing subset of *Mycobacterium tuberculosis* (*M.tb*) strains that is resistant to existing anti-TB drugs. In affected immune-competent individuals with no active disease, the bacilli remain protected at the primary sites of infection in granulomas that provide immunologic and physical barrier to ensure bacterial survival, and may promote the development of persistent bacteria or persisters, reduced drug penetration, and diminished antimicrobial killing until loss of immune protection reactivates disease. A leading hypothesis is that persisters develop as an adaptation to host immune pressure within granulomatous lesions. Under this hypothesis, persisters represent phenotypic variants which, due to immunologic stress, enter a slow-sporadic, or non-growing state which makes them tolerant to antimicrobial killing (McCune et al., 1957). This hypothesis suggests that a strategy to accelerate cure is to prevent entry into the poorly growing persister phenotypic state and to reactivate quiescent lesions by transient immune modulation. This transient reactivation and subsequent antimicrobial killing, or "wake 'em and whack 'em" strategy, has been recently advocated as one of the novel approaches to combat the spread of tuberculosis by the global *Stop TB Partnership* (Robertson et al., 2012), which, in collaboration with the World Health Organization, recently set the goal of eliminating tuberculosis world-wide by 2050.

The mechanisms by which *M.tb* persisters modulate host responses to ensure survival remain unclear. It is believed that a balance between pro-inflammatory cytokines such as IL-12, IFN-γ, and TNF-α, and anti-inflammatory cytokines such as IL-10 plays a role (Cilfone et al., 2013; Marino et al., 2015). An effective reactivation strategy would therefore aim at tipping this balance by either suppressing pro-inflammatory responses, or promoting anti-inflammatory responses, or both. In fact, an increased incidence of tuberculosis has been noted among patients on TNF-α inhibitors (Salgado and Gomez-Reino, 2011), and several laboratory and human clinical studies have demonstrated the efficacy of adding TNF-α inhibitors (TNF-Is) to antibacterial chemotherapy for TB (Wallis et al., 2004; Skerry et al., 2012); TNF neutralization also induces reactivation in nonhuman primates with latent tuberculosis infection (Lin et al., 2010). However in this model, TNF neutralization also alters chemokine receptor expression, and impaired cellular recruitment,

---

resulting in a disparate degree of extra-pulmonary disease. More importantly, at least in a third of animals, reactivation was not achieved following anti-TNF treatment, indicating that TNF may not be a critical factor in maintaining persisters (Lin et al., 2010).

In efforts to block pro-inflammatory responses, we recently showed that tofacitinib, a Janus kinase (JAK) inhibitor that was FDA-approved in 2012 for treating rheumatoid arthritis and ulcerative colitis (Traynor, 2012; Sandborn et al., 2012), blocked immune containment and promoted bacterial replication during chronic TB in the mouse paucibacillary model in the absence of anti-TB drugs (Maiga et al., 2012). Tofacitinib targets JAK3 (IC$_{50}$ 2 nM) and to a lesser degree JAK2 (IC$_{50}$ 20 nM) (Pesu et al., 2008). Inhibition of JAK3 reduces responsiveness to multiple pro-inflammatory cytokines including IL-2, IL-4, IL-15, and IL-21. In doing so tofacitinib inhibits the maturation of CD4$^+$CD25$^+$ (IL-2 receptor-bearing) T$_{eff}$ cells, though it appears to spare CD4$^+$CD25$^+$ T$_{reg}$ function (Sewgobind et al., 2010). Inhibition of JAK2 blocks responsiveness to IL-6 and IFN-γ. In this study, in order to adopt the "wake-'em to whack 'em" strategy for reducing TB treatment times, we evaluated tofacitinib as an adjuvant, host-directed therapy for TB while simultaneously treating with the standard anti-TB antibiotics for six months.

2. Materials and Methods

2.1. Animals, Drugs, and Bacteria

Six week-old female BALB/c (Charles River, MD, USA) and C3HeB/FeJ (Jackson Laboratories, ME, USA) mice were used with three mice per time point (PK studies), five mice per time point (chemotherapy studies), and 10 mice per regimen (relapse studies). Procedures were approved by the Johns Hopkins University Animal Care and Use Committee. Tofacitinib was purchased from LC Laboratories (Woburn, MA, USA) and administered by oral gavage in 0.5% (w/v) carboxymethylcellulose (Sigma-Aldrich, MO, USA) and 0.025% (vol/vol) Tween-20 (Sigma-Aldrich, MO, USA). All other drugs were obtained and used in doses as previously described (Gupta et al., 2013). They were administered by oral gavage in a total volume of 0.2 mL water. *M.tb* strain H37Rv was cultured at 37 °C in Middlebrook 7H9 broth (Becton-Dickinson, NJ, USA) supplemented with 10% (vol/vol) oleic acid–albumin–dextrose-catalase (OADC Becton-Dickinson, NJ, USA), 5% (vol/vol) glycerol and 0.05% (vol/vol) Tween-80 (Sigma-Aldrich, MO, USA). Susceptibility testing to isoniazid and rifampin (both obtained from Sigma-Aldrich, MO, USA) was performed using the microplate alamar blue assay (MABA) (Cho et al., 2015).

2.2. Pharmacokinetic Study

Rifampin was administered to mice at 10 mg/kg/day for seven days to achieve CYP3A and P-glycoprotein induction (Matheny et al., 2004). Tofacitinib was then administered in two doses 6 h apart for a total dose of 15, 22.5 or 30 mg/kg; the second dose was co-administered with rifampin at 10 mg/kg. Blood was collected from mice at 1, 2, 3, 4, 6, 7, 8, 10, 12 and 24 h post-administration of the first dose of tofacitinib. Serum samples were separated by centrifugation and stored at −80 °C until analysis. Drug levels were measured using an AB-Sciex QTrap 5500 LC/MS/MS (MA, USA) using 0.1% formic acid in deionized water (mobile phase A) and 0.1% formic acid in acetonitrile (mobile phase B) at a flow rate of 200 μl/min with an XTerra® MS column (C$_{18}$, 2.1 mm × 50 mm, particle size 3.5 μm, Waters Corporation, MA, USA). Quantitation of drug levels was performed using m/z transitions of 823.1/791.2 for rifampin and 313.4/149.1 for tofacitinib, and the chromatograms were analyzed using the Multiquant 2.1 software from AB-Sciex (MA, USA).

2.3. TB Chemotherapy Models

A mouse model of chronic TB was used for this study (Rosenthal et al., 2012). Mice were infected with *M.tb* H37Rv by aerosol (using

the Glas-Col inhalation exposure system, IN, USA) to implant 2 log$_{10}$ CFUs on day 1, and five mice were sacrificed the day after infection (time point: week −8 of drug treatment) to determine bacterial implantation. Treatment was initiated 8 weeks post-infection (time point: day 0), when the lung bacterial load stabilized at around 6 log$_{10}$ CFUs for BALB/c mice and 5 weeks post-infection when the lung bacterial burden was around 8.5 log$_{10}$ CFUs for C3HeB/FeJ mice (see Table S1 for BALB/c mouse experimental scheme). Treatment regimens were administered 5 days per week. Control regimens were no drug treatment and the standard short-course regimen: two months (the intensive phase) of daily isoniazid (H), rifampin (R) and pyrazinamide (Z) followed by 4 months (the continuation phase) of daily isoniazid and rifampin. The two test regimens for BALB/c study included the following changes to the standard treatment: the addition of tofacitinib and the replacement of pyrazinamide with tofacitinib. In the C3HeB/FeJ mouse study, only the addition of tofacitinib to the standard treatment was used. Five mice from each treatment group were sacrificed every 4 weeks post-treatment's initiation for lung CFU assessment. To assess the impact of discontinued treatment on relapse, drug administration was stopped for 10 mice in each group after 4 and 5 months of treatment for BALB/C study, and after 3 and 4 months of drug treatment for C3HeB/FeJ study. These mice, as well as 10 mice from each group that completed the full 6 months of treatment, were kept for an additional 3 months after ending treatment, at which point the mice were sacrificed for lung CFU assessment. Study endpoints included lung CFU counts, time to culture-negative status, and proportion of relapse (culture-positive lungs 3 months after ending treatment).

2.4. Cytokine Responses

Bone marrow-derived macrophages (BMDM) cells from BALB/c and C3HeB/FeJ mice were isolated following published protocol (Skinner et al., 1994) and infected with H37Rv for 2 h at a multiplicity of infection (MOI) of 1:10. Cells were washed and resuspended in MEM media (Life Technologies, CA, USA) overnight with or without treatment with tofacitinib at 300 nM. TNF-α and interleukin-1 beta (IL-1β) were measured 24, 48 and 96 h later by ELISA (R&D Systems, MN, USA). The data shown represent three biological and three technical replicates.

2.5. Statistical Analysis

Lung CFU counts (x) were log-transformed as log$_{10}$ (x + 1) prior to analysis. The Mann–Whitney *U* test was used to determine statistical significance between groups. To determine the differences in cytokine responses between BMDMs of the two different mouse strains, data were analyzed by two-way ANOVA with the Bonferroni's test applied to correct for multiple comparisons. Data analyses, including pharmacokinetic analyses, were performed with Prism 6.0 (GraphPad Software, CA, USA), and measures of variations expressed as ±SD.

3. Results

3.1. Pharmacokinetics of Tofacitinib and Rifampin Co-Administration

Because of the known tofacitinib-rifampin drug-drug interaction due to rifampin-mediated CYP3A4 induction, we first conducted a PK study to establish effective rifampin and tofacitinib doses in mice for drug co-administration. The concentration of tofacitinib required to inhibit JAK tyrosine kinase activity is 100 nM (31.2 ng/mL), and treatment with recommended doses achieves an AUC$_{0-24}$ of ~3250 nM·H (1014 ng/mL·H) with an elimination half-life of ~3 h (Dowty et al., 2014). First we assessed the effect of chronic rifampin exposure on tofacitinib levels. Rifampin was administered daily for seven days prior to a one-day co-administration of tofacitinib and rifampin. Since rifampin is only dosed once daily and tofacitinib twice, the first dose

of tofacitinib was administered and followed 6 h later by the second dose in conjunction with rifampin. After steady state rifampin exposure, the peak serum concentration achieved by all three doses of tofacitinib tested was 500–800 ng/mL, well above the concentration required to inhibit JAK tyrosine kinase activity (100 nM or 31.2 ng/mL). With rifampin pre-treatment and co-administration, the 24-hour area under the curve (AUC_{0-24}) values for tofacitinib were 2380 ng/ml·H, 5074 ng/ml·H, and 5156 ng/ml·H for 15, 22.5 and 30 mg/kg/day of tofacitinib, respectively (Fig. 1A). All of these tofacitinib AUC_{0-24} values compared favorably with typical human AUC_{0-24} achieved by the drug (1014 ng/mL·H). Interestingly, we observed increased tofacitinib levels in mouse serum on the second of the two daily doses, namely the dose that was co-administered with rifampin at t = 6 h. This may be due to relative saturation of the liver clearance enzymes by rifampin on this second dose.

Next we assessed the impact of tofacitinib on rifampin levels. Co-administration of tofacitinib with rifampin had only a modest impact on rifampin AUC_{0-18} values which were 77.2, 93.1 and 102.9 g/ml·H for mice that received 15, 22.5 and 30 mg/kg/day of tofacitinib, respectively, and it had no effect on the serum concentration of rifampin (Fig. 1B). These data suggest that tofacitinib could be administered with the standard TB chemotherapy regimen without drug–drug interactions adversely affecting drug levels. Based on these data, we selected a tofacitinib dose of 30 mg/kg/day given in two divided doses as it gave an elimination half-life closest that that in humans, achieved serum
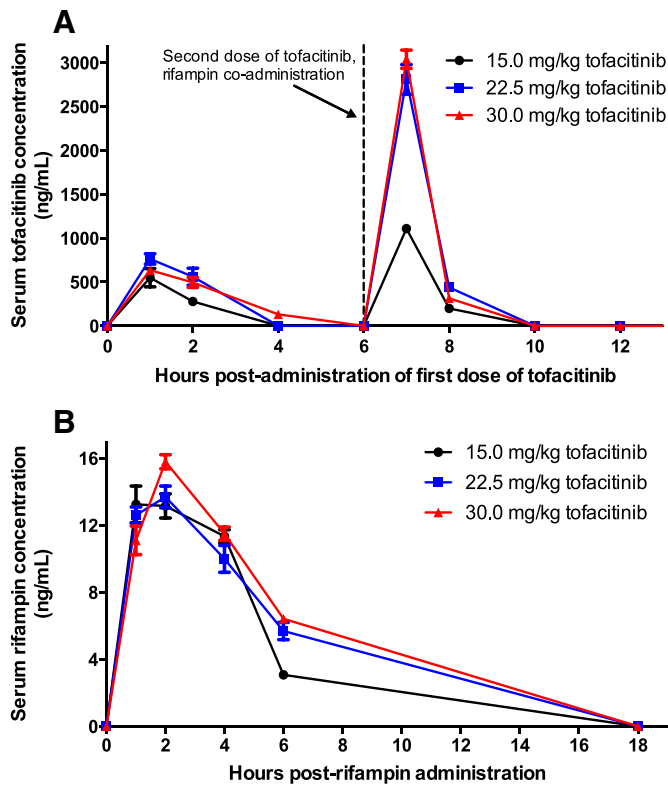

Fig. 1. A: Mouse serum concentrations of tofacitinib. Mouse serum concentrations of tofacitinib after dosing at 15, 22.5 and 30 mg/kg administered at t = 0 h and t = 6 h. A single dose of 10 mg/kg of rifampin was also administered at t = 6 h. The resulting tofacitinib area under curve concentrations (0–24 h) were 2380, 5074, and 5156 ng/ml·H, for the three respective doses. All mice were pre-treated daily for seven days with 10 mg/kg/day of rifampin to induce CYP3A4. B: Mouse serum concentrations of rifampin. Mouse serum concentrations of rifampin after dosing at 10 mg/kg at t = 0 h with tofacitinib 15, 22.5 and 30 mg/kg given at t = −6 h and t = 0 h. The resulting rifampin area under curve concentrations (0–18 h) were 77, 93, and 103 μg/ml·H for the respective co-administered tofacitinib dose. All mice were pre-treated daily for seven days with 10 mg/kg/day of rifampin to induce CYP3A4.

levels capable of inhibiting JAK tyrosine kinase activity for a reasonable portion of the 24-hour treatment cycle, and did not adversely affect rifampin levels (Cohen et al., 2010). The dose selected for our study apparently leads to an average exposure in mice at least three to five times higher than exposure for patients with rheumatoid arthritis on 10 mg per day dose. However, the concentration of tofacitinib 2 h after the dose is approximately 250–500 ng/mL with or without co-administration of rifampin, at all doses of tofacitinib tested, suggesting rapid hepatic and renal clearance, similar to seen in pharmacokinetic studies in humans (Dowty et al., 2014).

3.2. Addition of Tofacitinib to Six-Month Standard TB Chemotherapy

In this study, we utilized the 6-month chronic mouse model of TB, and standard chemotherapy (Std-Rx) consisting of 2 months of isoniazid (H), rifampin (R) and pyrazinamide (Z) treatment, followed by 4 months of isoniazid and rifampin (2HRZ/4HR) to address whether inclusion of tofacitinib as an adjunctive to standard chemotherapy (2HRZT/4HRT) may shorten TB treatment duration in both immuno-competent BALB/c mice, and in C3HeB/FeJ mice that are deficient at the *sst1* ("supersusceptibility to tuberculosis") locus. Based on recent reports that pyrazinamide may inhibit host inflammatory responses (Manca et al., 2013), we also tested substitution of pyrazinamide with tofacitinib in Std-Rx (2HRT/4HR) (Supplementary Table 1).

3.2.1. BALB/c Mice

We infected BALB/c mice by the aerosol route with a day-1 lung implantation of 2.40 (standard deviation [SD] 0.08) $\log_{10}$ CFUs. Drug treatments commenced 8 weeks after infection, when the bacterial lung burden was at 6.43 (SD 0.31) $\log_{10}$ CFUs. No significant differences in the different treatment groups were seen during the first eight weeks. However, at week 16 of treatment, mice treated with 2HRZT/4HRT showed significantly lower CFU counts compared to Std-Rx of 2HRZ/4HR, with p values of 0.013 (Fig. 2A and Supplementary Table 2). Mice receiving 2HRZT/4HRT had no detectable bacteria in the lungs after 16 weeks of treatment, whereas the 2HRT/4HR and Std-Rx groups required 24 weeks, to reach the same endpoint. Replacement of pyrazinamide with tofacitinib (2HRT/4HR versus 2HRZ/4HR) improved bacterial killing between 12 to 16 weeks of treatment (Fig. 2A). Although pyrazinamide is known to be effective against poorly replicating or semi-dormant bacilli, this suggests that reactivation mediated by tofacitinib may be most active when administered together with pyrazinamide during the bactericidal phase of treatment (Fig. 2A between the t = 0 and 4 weeks).

Our earlier histopathology studies showed that lungs from BCG immunized, tofacitinib-treated mice challenged with H37Rv showed moderate lesions of leukocyte aggregation at 4 weeks of tofacitinib treatment compared to BCG immunized, untreated mice challenged with H37Rv, confirming bacterial reactivation mediated by tofacitinib (Maiga et al., 2012). It was interesting to note that the relapse rate did not differ among mouse groups receiving Std-Rx alone or those receiving it in addition to tofacitinib. In contrast, replacement of pyrazinamide by tofacitinib (2HRT/4HR group) was detrimental when treatment was stopped at month 4 with a higher relapse rate in the 2HRT/4HR group (80%) compared to the Std-Rx group (20%) (Table 1).

3.2.2. C3HeB/FeJ Mice

C3HeB/FeJ inbred mice are extremely susceptible to *M.tb* due to naturally occurring mutations in the intracellular pathogen resistance 1 (*Ipr1*) isoform of the interferon-inducible 75 (*Ifi75*) gene (Pan et al., 2005). Infected mice develop marked lung pathology, with necrotic granulomas more closely resembling human lesions that harbor latent bacilli ("Kramnik mouse model"). We therefore tested the efficacy of tofacitinib as an adjunct to chemotherapeutic drugs in infected C3HeB/FeJ mice. We infected the mice by the aerosol route with a day
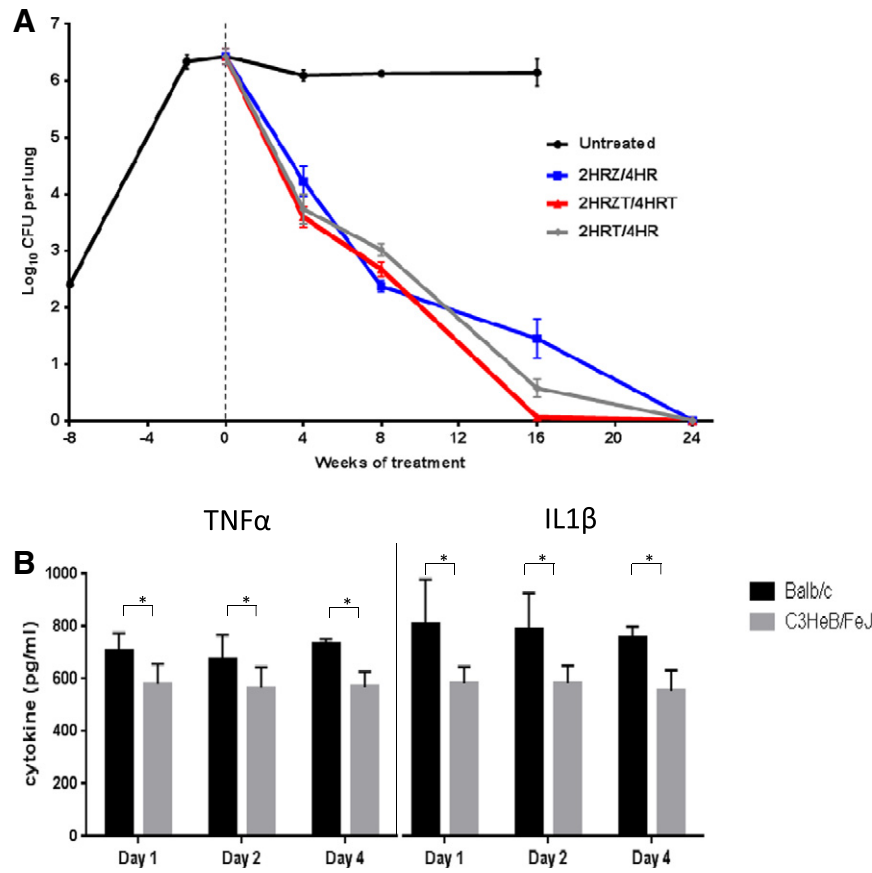
Fig. 2. A: Growth of *M.tb* in BALB/c mouse lungs during treatment. BALB/c mouse mean lung $\log_{10}$ CFU counts for the dosing regimens shown in the inset. Mice infected by the aerosol route achieved a day-1 lung implantation of 2.40 (standard deviation [SD] 0.08) $\log_{10}$ CFUs, and 8 weeks after infection at the initiation of treatment the bacterial lung burden was at 6.43 (SD 0.31) $\log_{10}$ CFUs. No differences across the groups were seen during the first 8 weeks. However, mice treated with 2HRZT/4HRT had lower lung bacterial burden than mice treated with the Std-Rx of 2HRZ/4HR at week 16 (P = 0.013). The group receiving 2HRT/4HR showed lower but not statistically significant CFU counts at 16 weeks (P = 0.0937). B: Cytokine levels from BALB/c and C3HeB/FeJ bone marrow-derived macrophages (BMDMs) following infection with *M.tb* and tofacitinib treatment. Differences in cytokine levels of infected BALB/c and C3HeB/FeJ bone marrow-derived macrophages (BMDMs) upon infection with *M.tb*. The BMDMs of BALB/c and C3HeB/FeJ BMDMs were infected with H37Rv for 2 h at a multiplicity of infection (MOI) of 1:10. TNF-α and IL-1β levels were measured by ELISA 24, 48 and 96 h later. Data shown here, which represents three biological and technical replicates, were analyzed by two-way ANOVA with the Bonferroni's test applied to correct for multiple comparisons. Despite similar baseline values (i.e. undetectable TNFα levels and approximately 250 pg/ml IL-1β levels), infected BALB/c mice showed consistent and significantly higher levels of both cytokine secretions when compared to C3HeB/FeJ mice. Addition of tofacitinib (300 nM) to uninfected or infected cells did not alter the cytokine levels (not shown). An asterisk (*) indicates p < 0.005.

1 lung implantation of 2.56 (SD 0.10) $\log_{10}$ CFUs. Five weeks after infection the bacterial lung burden reached 8.78 (SD 0.63) $\log_{10}$ CFUs with mice becoming lethargic at that point. In these mice, during the five months of treatment with 2HRZ/3HR versus 2HRZT/3HRT, no difference in lung CFU burdens was observed between the two groups (Supplementary Table 3), unlike observations in BALB/c mice.

Table 1
Proportions of BALB/c mice with relapse 3 months post-treatment.

Duration of treatment	Proportion of mice with detectable bacilli in the lungs		
	2HRZ/4HR	2HRZT/4HRT	2HRT/4HR
4 months (M4 + 3)	2/10	3/10	8/10
5 months (M5 + 3)	0/10	0/10	2/10
6 months (M6 + 3)	0/10	0/10	0/10

H: isoniazid at 25 mg/kg/day; R: rifampin at 10 mg/kg/day; Z: pyrazinamide at 150 mg/kg/day; T: tofacitinib at 30 mg/kg/day; and + 3: plus three months without treatment. The columns slow the three treatment groups of BALB/c mice evaluated in this study. After receiving treatment for 4, 5, or 6 months, groups of ten mice were removed from treatment and held for 3 additional months. Following 3 months of no treatment, these mice were sacrificed and the lung homogenates subjected to CFU counting. The numbers of mice with relapse (with any detectable lung CFU) are shown.

In addition, no difference was seen in 3-month relapse rates post-treatment.

3.3. Determination of Isolates' Resistance Patterns During Treatment in the BALB/c Chronic Model

Colonies were isolated from different groups of BALB/c mice in order to assess their resistance profiles after four months of treatment. All isolates remained fully susceptible to isoniazid and rifampin with minimum inhibitory concentrations of 0.04 μg/ml and 0.25 μg/ml, respectively, indicating that no genotypic resistance developed during mice treatment. We also determined the minimal inhibitory concentration of tofacitinib against wild type H37Rv to be >64 μg/ml, a level significantly above the peak tofacitinib serum concentration in mice during our PK experiments (3 μg/ml). In this regard, it is to be noted that single drug treatment leads to significantly increased numbers of drug-resistant colonies in infected C3HeB/FeJ mice compared to BALB/c mice (Driver et al., 2012).

3.4. Cytokine Responses to Tofacitinib From Infected BMDM of BALB/c and C3HeB/FeJ Mice

In order to better understand the lack of activity of tofacitinib adjunctive therapy in C3HeB/FeJ mice, we isolated BMDMs from both

BALB/c and C3HeB/FeJ mice, infected them with *M.tb* in culture, and evaluated their pro-inflammatory cytokine responses. Cells from both mouse strains showed similar levels of cytokine secretion in the absence of infection (undetectable levels of TNFα and approximately 250 pg/mL of IL-1β). However, following *M.tb* infection BMDM from C3HeB/FeJ mice, cells expressed significantly weaker cytokine responses than BALB/c mice (Fig. 2B). C3HeB/FeJ macrophages secreted 580 (±87) pg/ml of TNF-α versus 705 (±37) pg/ml from BALB/c cells. For IL-1β, C3HeB/FeJ macrophages secreted 583 (±64) pg/ml versus 811 (±67) pg/ml from BALB/c, findings which are consistent with earlier reports in a mouse LPS-challenge model (Ghoreschi et al., 2011). Addition of tofacitinib to uninfected or infected cells did not alter the cytokines expressed by BMDMs from either source. These data reveal that following *M.tb* infection C3HeB/FeJ mice mount a reduced pro-inflammatory response, which appears to be functional consequence of inactivation of the *intracellular pathogen resistance* 1 (*ipr1*) gene in these mice. Because tofacitinib acts by reducing target cell responses following pro-inflammatory cytokine binding, the lack of efficacy of tofacitinib in C3HeB/FeJ mice may stem from the fact that these mice have lower pro-inflammatory cytokine levels to start with and therefore also a reduced JAK signal to be inhibited by tofacitinib. Ipr1 gene regulates apoptotic cell death in *M.tb*-infected macrophages (Pan et al., 2005). Hence it is also likely that differential cell death via apoptosis accounts for differences in cytokine expression of BMDM from the two sources.

4. Discussion

In this study, we used a well-established mouse model of chronic *M.tb* infection to evaluate the addition of tofacitinib to 6-month Std-Rx for TB. Our data suggest that addition of tofacitinib, which is an orally administered, FDA-approved JAK inhibitor, may be beneficial in TB treatment by reducing the time to apparent sterilization achievable with Std-Rx. BALB/c mice receiving 2HRZT/4HRT showed complete lung clearance of *M.tb* at 16 weeks of treatment while Std-Rx alone required 24 weeks to achieve apparent sterilization. A major strength of this study is that we tested the addition of a host-directed therapeutic agent head-to-head against a validated, full-course, standard regimen for TB and found a beneficial effect. While other host-directed therapies have shown enhanced clearance together with single antibiotics or other forms of partially effective therapy, improving upon full Std-Rx by addition of immunomodulatory drugs is more difficult to achieve, but is ultimately a goal that will be required for advancing host-directed therapies into human clinical research. It is to be pointed out here that the dose selected for our study leads to an average exposure in mice at least three to five times higher than exposure for patients with rheumatoid arthritis on a recommended dose of 10 mg per day. Even though efficacy of tofacitinib is dose-related in human rheumatoid arthritis (Lee et al., 2014), higher doses have not been recommended due to increased risk of serious infections and malignancies. During the study period, we did not observe any adverse effects in mice at the higher dose, suggesting that pharmacokinetics and drug–drug interactions in mice are rather poor predictors of events in humans.

Interestingly, although tofacitinib significantly accelerated the time to apparent lung sterilization when added to Std-Rx in BALB/c mice, it did not alter the time to achieve relapse-free cure, which required five months in both the Std-Rx and 2HRZT/4HRT treatment groups (Table 1). This suggests that despite achieving apparent clearance in mouse lungs at 16 weeks, the 2HRZT/4HRT regimen was unable to achieve true sterilization until the five-month time point. This finding suggests that the acceleration of therapy with tofacitinib may not translate into a more rapid non-relapsing cure. It is also reminiscent of the well-studied apparent sterile state achieved in the Cornell mouse latency model in mice treated with isoniazid and pyrazinamide for 12 weeks (McCune and Tompsett, 1956), and hence may not reflect the ability of humans to achieve sterilization because humans are more resistant to *M.tb* than mice and can mount bactericidal immunity.

By inhibiting JAK3- and to a lesser degree JAK2-mediated phosphorylation of activated cytokine receptors and the subsequent recruitment of STAT transcription factors, tofacitinib reduces responsiveness to circulating pro-inflammatory cytokines (primarily IL-2, IL-4, IL-15, and IL21 for JAK3; and IFN-γ, IL-6, IL-12 and IL-23 for JAK2) (Pesu et al., 2008). By blocking cytokine-mediated T cell activation, tofacitinib also inhibits T_{eff} cell differentiation but has limited action on T_{reg} function (Sewgobind et al., 2010). Tofacitinib also blocks secretion of TNF-α and IL-1β in mice following LPS challenge (Ghoreschi et al., 2011), and by human dendritic cells stimulated by LPS (Kubo et al., 2014), a finding which we observed in *M.tb* infected BMDM (Fig. 2B). Our findings suggest that immunomodulatory drugs such as tofacitinib could block immune containment of *M.tb* and promote bacterial replication that can be targeted by standard drugs. It is likely that other similar immunomodulatory drugs may perform even better.

While the anti-inflammatory effect of tofacitinib led to an acceleration of *M.tb* clearance in wild-type BALB/c mice receiving 2HRZT/4HRT, when the same regimen was used on C3HeB/FeJ mice, which harbor mutations in the *Ipr1* gene, it had no effect, suggesting that the effect of tofacitinib is dependent on the host biology and immune response. BALB/c mice are preferred as the traditional validated animal model for TB drug evaluation. Many studies in BALB/c mice have been directly translated to human trials with good correlation. On the other hand, C3HeB/FeJ mice are much more susceptible to *M.tb* infection, and serve as experimental models for lesions of lung necrosis (Driver et al., 2012). The absence of tofacitinib activity in C3HeB/FeJ mice is also consistent with earlier observations that mice with mutations in the sst1 locus mount significantly reduced IL-6 and IL-1β responses as well as $CD4^+CD25^+$ T_{eff} cell responses during *M.tb* infection (Pichugin et al., 2009; Yan et al., 2007). Since *sst1*-deficient mice display blunted pro-inflammatory cytokine induction and reduced IL-2-receptor (CD25)-mediated T_{eff} maturation, it is not surprising that tofacitinib, which blocks receptor function for these key cytokines, showed little effect in these mice. While tofacitinib (a broad cytokine activation inhibitor) had no activity in C3HeB/FeJ mice, Skerry et al. recently observed significant acceleration of *M.tb* clearance with the addition of etanercept (a specific TNF-α receptor antagonist) to Std-Rx (Skerry et al., 2012). Hence, it is possible that the nature of the granulomatous lesions in C3HeB/FeJ mice, which are necrotic and hypoxic compared with those of BALB/c mice, prevents action of tofacitinib but allows action of other anti-inflammatory agents such as etanercept. Tofacitinib blocks IL-10-mediated feedback inhibition on pro-inflammatory cytokine transcription in macrophages (Pattison et al., 2012). *In silico* studies show that a balance of TNF-α and IL-10 concentrations is essential to *M.tb* infection control within a single granuloma (Cilfone et al., 2013). In fact, in the C3HeB/FeJ mouse model of TB, mice treated with anti-inflammatory drugs such as ibuprofen showed decreased lung lesions and bacillary load, and improved survival (Vilaplana et al., 2013). Massive neutrophilic infiltration is also likely a key determinant of the development of the necrotic lesions in C3HeB/FeJ mice and of susceptibility to TB (Marzo et al., 2014). The above factors could determine different lung pathology and outcomes in C3HeB/FeJ mice compared to the BALB/c mice. It is to be noted that infected C3HeB/FeJ mice are also resistant to monotherapy including isoniazid, pyrazinamide, and clofazimine (Driver et al., 2012; Irwin et al., 2014), and that administration of clofazimine prior to the formation of hypoxic, necrotic granulomas leads to therapeutic efficacy (Irwin et al., 2014). Irwin et al. (Irwin et al., 2014) show that the differential activity of clofazimine in BALB/c and C3HeB/FeJ mice is specifically related to the granulomatous pathology in the lungs of these mice, and not due to differences in immune function between mouse strains, since clofazimine is also effective in immunocompromised, interferon-γ knockout mice. To study the role of hypoxic granulomas in the attenuated effect of tofacitinib in C3HeB/FeJ mice, our future studies will therefore evaluate the efficacy of 2HRZT/4HRT regimen at earlier time points post-infection (~3 weeks), when lesions

containing caseous necrotic material are absent. Our future studies will also evaluate the efficacy of adjunctive tofacitinib therapy at exposures similar to doses recommended in humans.

5. Conclusion

Our findings suggest that targeting the JAK pathway may accelerate TB treatment times when used as an adjunctive host-directed therapy together with standard anti-tuberculous chemotherapy, even though this may not lead to more rapid non-relapsing cure. Our data also suggest that the nature of granulomatous lesions and host immunity may influence responsiveness to tofacitinib.

Author Contributions

Conception and design: M.M., B.A.A., S.L., M.C.M., F.B. and W.R.B.; acquisition of data: M.M., M.C.M., B.A.A., and LC; analysis and interpretation: M.M., B.A.A., LC, S.P., and M.C.M.; and drafting the manuscript: M.M., B.A.A., S.P., S.L., F.B. and W.R.B.

Financial Disclosure

The authors declare no financial or potential conflicts of interest.

Acknowledgments

Appendix A. Supplementary Data

Supplementary data to this article can be found online at http://dx. doi.org/10.1016/j.ebiom.2015.07.014.

References

Cho, S., Lee, H.S., Franzblau, S., 2015. Microplate alamar blue assay (MABA) and low oxygen recovery assay (LORA) for *Mycobacterium tuberculosis*. Methods Mol. Biol. 1285, 281–292.

Cilfone, N.A., Perry, C.R., Kirschner, D.E., Linderman, J.J., 2013. Multi-scale modeling predicts a balance of tumor necrosis factor-alpha and interleukin-10 controls the granuloma environment during *Mycobacterium tuberculosis* infection. PLoS One 8, e68680.

Cohen, S., Zwillich, S.H., Chow, V., Labadie, R.R., Wilkinson, B., 2010. Co-administration of the JAK inhibitor CP-690,550 and methotrexate is well tolerated in patients with rheumatoid arthritis without need for dose adjustment. Br. J. Clin. Pharmacol. 69, 143–151.

Dowty, M.E., Jesson, M.I., Ghosh, S., Lee, J., Meyer, D.M., Krishnaswami, S., Kishore, N., 2014. Preclinical to clinical translation of tofacitinib, a Janus kinase inhibitor, in rheumatoid arthritis. J. Pharmacol. Exp. Ther. 348, 165–173.

Driver, E.R., Ryan, G.J., Hoff, D.R., Irwin, S.M., Basaraba, R.J., Kramnik, I., Lenaerts, A.J., 2012. Evaluation of a mouse model of necrotic granuloma formation using C3HeB/FeJ mice for testing of drugs against *Mycobacterium tuberculosis*. Antimicrob. Agents Chemother. 56, 3181–3195.

Ghoreschi, K., Jesson, M.I., Li, X., Lee, J.L., Ghosh, S., Alsup, J.W., Warner, J.D., Tanaka, M., Steward-Tharp, S.M., Gadina, M., Thomas, C.J., Minnerly, J.C., Storer, C.E., Labranche, T.P., Radi, Z.A., Dowty, M.E., Head, R.D., Meyer, D.M., Kishore, N., O'Shea, J.J., 2011. Modulation of innate and adaptive immune responses by tofacitinib (CP-690,550). J. Immunol. 186, 4234–4243.

Gupta, S., Tyagi, S., Almeida, D.V., Maiga, M.C., Ammerman, N.C., Bishai, W.R., 2013. Acceleration of tuberculosis treatment by adjunctive therapy with verapamil as an efflux inhibitor. Am. J. Respir. Crit. Care Med. 188, 600–607.

Irwin, S.M., Gruppo, V., Brooks, E., Gilliland, J., Scherman, M., Reichlen, M.J., Leistikow, R., Kramnik, I., Nuermberger, E.L., Voskuil, M.I., Lenaerts, A.J., 2014. Limited activity of clofazimine as a single drug in a mouse model of tuberculosis exhibiting caseous necrotic granulomas. Antimicrob. Agents Chemother. 58, 4026–4034.

Kubo, S., Yamaoka, K., Kondo, M., Yamagata, K., Zhao, J., Iwata, S., Tanaka, Y., 2014. The JAK inhibitor, tofacitinib, reduces the T cell stimulatory capacity of human monocyte-derived dendritic cells. Ann. Rheum. Dis. 73, 2192–2198.

Lee, E.B., Fleischmann, R., Hall, S., Wilkinson, B., Bradley, J.D., Gruben, D., Koncz, T., Krishnaswami, S., Wallenstein, G.V., Zang, C., Zwillich, S.H., Van Vollenhoven, R.F., 2014. Tofacitinib versus methotrexate in rheumatoid arthritis. N. Engl. J. Med. 370, 2377–2386.

Lin, P.L., Myers, A., Smith, L., Bigbee, C., Bigbee, M., Fuhrman, C., Grieser, H., Chiosea, I., Voitenek, N.N., Capuano, S.V., Klein, E., Flynn, J.L., 2010. Tumor necrosis factor neutralization results in disseminated disease in acute and latent *Mycobacterium tuberculosis* infection with normal granuloma structure in a cynomolgus macaque model. Arthritis Rheum. 62, 340–350.

Maiga, M., Lun, S., Guo, H., Winglee, K., Ammerman, N.C., Bishai, W.R., 2012. Risk of tuberculosis reactivation with tofacitinib (CP-690550). J. Infect. Dis. 205, 1705–1708.

Manca, C., Koo, M.S., Peixoto, B., Fallows, D., Kaplan, G., Subbian, S., 2013. Host targeted activity of pyrazinamide in *Mycobacterium tuberculosis* infection. PLoS One 8, e74082.

Marino, S., Cilfone, N.A., Mattila, J.T., Linderman, J.J., Flynn, J.L., Kirschner, D.E., 2015. Macrophage polarization drives granuloma outcome during *Mycobacterium tuberculosis* infection. Infect. Immun. 83, 324–338.

Marzo, E., Vilaplana, C., Tapia, G., Diaz, J., Garcia, V., Cardona, P.J., 2014. Damaging role of neutrophilic infiltration in a mouse model of progressive tuberculosis. Tuberculosis (Edinb.) 94, 55–64.

Matheny, C.J., Ali, R.Y., Yang, X., Pollack, G.M., 2004. Effect of prototypical inducing agents on P-glycoprotein and CYP3A expression in mouse tissues. Drug Metab. Dispos. 32, 1008–1014.

McCune Jr., R.M., Tompsett, R., 1956. Fate of *Mycobacterium tuberculosis* in mouse tissues as determined by the microbial enumeration technique. I. The persistence of drug-susceptible tubercle bacilli in the tissues despite prolonged antimicrobial therapy. J. Exp. Med. 104, 737–762.

McCune, R.M., Lee, E., Deuschle, K., McDermott, W., 1957. Ineffectiveness of isoniazid in modifying the phenomenon of microbial persistence. Am. Rev. Tuberc. 76, 1106–1109.

Pan, H., Yan, B.S., Rojas, M., Shebzukhov, Y.V., Zhou, H., Kobzik, L., Higgins, D.E., Daly, M.J., Bloom, B.R., Kramnik, I., 2005. Ipr1 gene mediates innate immunity to tuberculosis. Nature 434, 767–772.

Pattison, M.J., Mackenzie, K.F., Arthur, J.S., 2012. Inhibition of JAKs in macrophages increases lipopolysaccharide-induced cytokine production by blocking IL-10-mediated feedback. J. Immunol. 189, 2784–2792.

Pesu, M., Laurence, A., Kishore, N., Zwillich, S.H., Chan, G., O'Shea, J.J., 2008. Therapeutic targeting of Janus kinases. Immunol. Rev. 223, 132–142.

Pichugin, A.V., Yan, B.S., Sloutsky, A., Kobzik, L., Kramnik, I., 2009. Dominant role of the sst1 locus in pathogenesis of necrotizing lung granulomas during chronic tuberculosis infection and reactivation in genetically resistant hosts. Am. J. Pathol. 174, 2190–2201.

Robertson, B.D., Altmann, D., Barry, C., Bishai, B., Cole, S., Dick, T., Duncan, K., Dye, C., Ehrt, S., Esmail, H., Flynn, J., Hafner, R., Handley, G., Hanekom, W., Van Helden, P., Kaplan, G., Kaufmann, S.H., Kim, P., Lienhardt, C., Mizrahi, V., Rubin, E., Schnappinger, D., Sherman, D., Thole, J., Vandal, O., Walzl, G., Warner, D., Wilkinson, R., Young, D., 2012. Detection and treatment of subclinical tuberculosis. Tuberculosis (Edinb.) 92, 447–452.

Rosenthal, I.M., Tasneen, R., Peloquin, C.A., Zhang, M., Almeida, D., Mdluli, K.E., Karakousis, P.C., Grosset, J.H., Nuermberger, E.L., 2012. Dose-ranging comparison of rifampin and rifapentine in two pathologically distinct murine models of tuberculosis. Antimicrob. Agents Chemother. 56, 4331–4340.

Salgado, E., Gomez-Reino, J.J., 2011. The risk of tuberculosis in patients treated with TNF antagonists. Expert. Rev. Clin. Immunol. 7, 329–340.

Sandborn, W.J., Ghosh, S., Panes, J., Vranic, I., Su, C., Rousell, S., Niezychowski, W., 2012. Tofacitinib, an oral Janus kinase inhibitor, in active ulcerative colitis. N. Engl. J. Med. 367, 616–624.

Sewgobind, V.D., Quaedackers, M.E., Van Der Laan, L.J., Kraaijeveld, R., Korevaar, S.S., Chan, G., Weimar, W., Baan, C.C., 2010. The Jak inhibitor CP-690,550 preserves the function of CD4CD25FoxP3 regulatory T cells and inhibits effector T cells. Am. J. Transplant. 10, 1785–1795.

Skerry, C., Harper, J., Klunk, M., Bishai, W.R., Jain, S.K., 2012. Adjunctive TNF inhibition with standard treatment enhances bacterial clearance in a murine model of necrotic TB granulomas. PLoS One 7, e39680.

Skinner, P.S., Furney, S.K., Jacobs, M.R., Klopman, G., Ellner, J.J., Orme, I.M., 1994. A bone marrow-derived murine macrophage model for evaluating efficacy of antimycobacterial drugs under relevant physiological conditions. Antimicrob. Agents Chemother. 38, 2557–2563.

Traynor, K., 2012. FDA approves tofacitinib for rheumatoid arthritis. Am. J. Health Syst. Pharm. 69, 2120.

Vilaplana, C., Marzo, E., Tapia, G., Diaz, J., Garcia, V., Cardona, P.J., 2013. Ibuprofen therapy resulted in significantly decreased tissue bacillary loads and increased survival in a new murine experimental model of active tuberculosis. J. Infect. Dis. 208, 199–202.

Wallis, R.S., Kyambadde, P., Johnson, J.L., Horter, L., Kittle, R., Pohle, M., Ducar, C., Millard, M., Mayanja-Kizza, H., Whalen, C., Okwera, A., 2004. A study of the safety, immunology, virology, and microbiology of adjunctive etanercept in HIV-1-associated tuberculosis. AIDS 18, 257–264.

Yan, B.S., Pichugin, A.V., Jobe, O., Helming, L., Eruslanov, E.B., Gutierrez-Pabello, J.A., Rojas, M., Shebzukhov, Y.V., Kobzik, L., Kramnik, I., 2007. Progression of pulmonary tuberculosis and efficiency of bacillus Calmette–Guerin vaccination are genetically controlled via a common sst1-mediated mechanism of innate immunity. J. Immunol. 179, 6919–6932.